Available online at www.sciencedirect.com
ScienceDirect
Simulation Modelling Practice and Theory 15 (2007) 1239–1258
SIMULATION MODELLING PRACTICE AND THEORY
www.elsevier.com/locate/simpat

Neuro-fuzzy MIMO nonlinear control for ceramic roller kiln

Nguyen Quoc Dinh *, Nitin V. Afzulpurkar

Industrial Systems Engineering, Asian Institute of Technology (AIT), P.O. Box 4, Klong Luang, Pathumthani 12120, Thailand

Received 26 October 2006; accepted 14 August 2007
Available online 25 August 2007

Abstract

Artificial neural networks (ANNs) and neuro-fuzzy systems (NFSs) have been widely used in modeling and control of many practical industrial nonlinear processes. However, most of them have concentrated on single-output systems only. In this paper, we present a comparative study using ANNs and co-active neuro-fuzzy inference system (CANFIS) in modeling a real, complicated multi-input–multi-output (MIMO) nonlinear temperature process of roller kiln used in ceramic tile manufacturing line. Using this study, we prove that CANFIS is better suited for modeling the temperature process in control phase. After that, a neural network (NN) controller has been developed to control the above mentioned temperature process due to a feedback control diagram. The designed controller performance is tested by a Visual C++ project and the resulting numerical data shows that this controller can work accurately and reliably when the roller kiln set-point temperature set changes.

Keywords: Ceramic roller kiln; Modeling; Control; Multi-input–multi-output nonlinear temperature process; Co-active neuro-fuzzy inference system

1. Introduction

One important industry related to construction field is ceramic tile manufacturing industry. Ceramic tiles are used to cover floor and pave walls for the industrial and civil construction project. Therefore, ceramic tile has to satisfy the qualities such as shape, size, durability, hardness and especially, deformation. In order to meet the rapidly developing demand about quantity, quality and prices as well as multiform character of ceramic tiles, there are several research teams currently trying to improve ceramic tile manufacturing technology such as Vieira et al. [12]. In fact, ceramic tile manufacturing line is a very complicated process with many stations such as grinding machine, spray-drying, pressing machine, vertical dryer, roller kiln, sorting line, packaging (Fig. 1). In this set of machines, performance of roller kiln is a key process which controls final tile quality. The tile quality can be measured by parameters such as flatness of surface, crack, durability and rigid character of the finished tiles. From Fig. 1, we can see that roller kiln is nearly the last station, hence, if there is

* Corresponding author. Tel.: +66 2 524 5693; fax: +66 2 524 5697.
E-mail address: nq_dinh2001@yahoo.com (N.Q. Dinh).

1569-190X/$ - see front matter © 2007 Elsevier B.V. All rights reserved.
doi:10.1016/j.simpat.2007.08.005

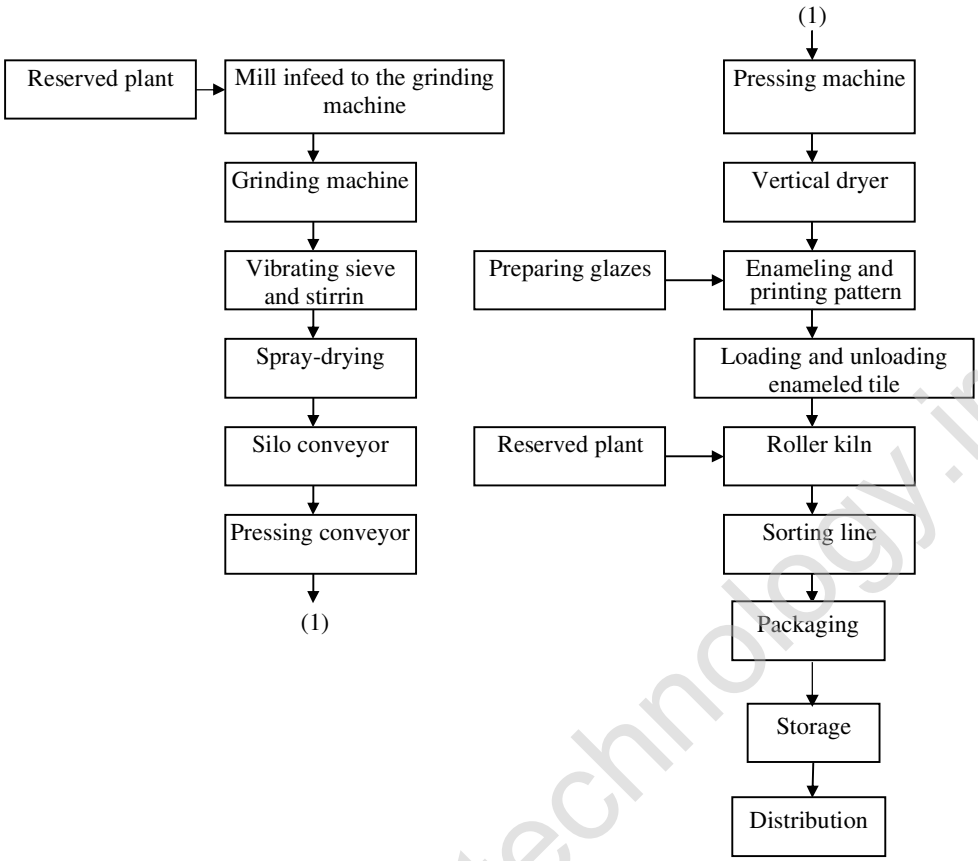

Fig. 1. Block diagram of ceramic tile manufacturing line.

any problem at this station then all efforts and materials of all preceding stations will be wasted. If temperature values in roller kiln do not follow accurately the reference curve, then many serious defects such as cracks and fractures, black heart, insufficient firing and overfiring, tonality variations of the glaze, size variations, planarity defects will occur in the finished ceramic tiles. Therefore, roller kiln is always expected to work accurately and reliably to meet all engineering requirements of finished product as much as possible.

In order to avoid the defects and obtain better quality for finished product, it is essential to improve the control for temperature process in roller kiln. This requires good controller design to make temperature process control in roller kiln as accurate as possible. To be able to control this temperature process, first, we have to build the controlled plant model using the process data collected from ceramic tile plant. Normally, there are two main approaches to construct the model of the plant. The first one is to develop the mathematical model directly from physical laws and relationships that govern plant processes. But sometimes, the knowledge about plant is not enough to derive the equations of the mathematical model or the equations are too complicated. In such cases, the second approach is to collect the input–output data of plant and this data is used to train NN or neuro-fuzzy model. In this paper, due to the complexity of physical behaviours of temperature process in roller kiln, the second approach is selected with off-line identification to develop the model of the studied nonlinear temperature process. After that, a real-time NN controller is designed to make the output temperature of roller kiln track the set-point values closely.

2. Description of the ceramic tile roller kiln temperature process

According to the temperature distribution, the whole roller kiln can be divided into six areas as shown in Fig. 2. Each area plays a specific role. In the kiln infeed area, water in the tile is evaporated to reach humidity of less than 1% of its weight. There is no heating and sintering in this area. Next, in pre-sintering area, air inside tiles is eliminated, hence, tile will avoid sponges and deformations as it is sintered. The sintering area

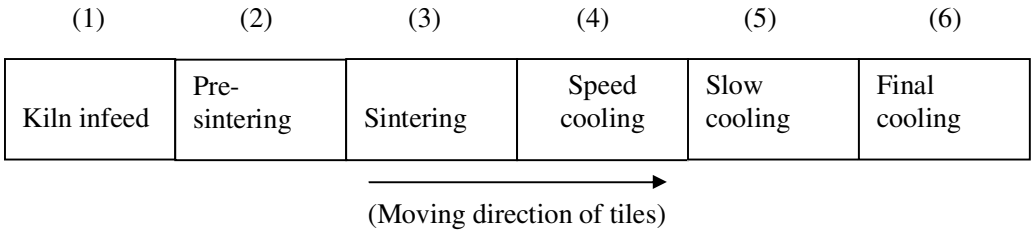

Fig. 2. Six areas of roller kiln.

is the most important because it decides all the temperature values inside the whole roller kiln. In this area, the maximum temperature of roller kiln is obtained. There are many firing nozzles and combustion chambers. Key parameters of the finished tile such as flatness, deformations, defects of glaze are decided in this area. After sintering, tiles are transported by roller to speed cooling area where temperature of kiln is rapidly reduced from maximum. In slow cooling area, changing temperature and pressure reduces volume of tiles considerably. In this area, all processes have to be carried out slowly and uniformly because glazing, shining level of surface and the perfect square shape of tiles depend on this area's temperature profile. Finally, after passing the slow cooling process, tiles return to the low temperature value in final cooling area. A graphical representation of ceramic roller kiln is shown in Fig. 3.

Actually, the temperature profile of roller kiln is very complicated. The main heating/cooling processes occurring in roller kiln can be listed as follows:

- Gas burning process in combustion chamber to generate heat.
- Heat absorbing process of cooling air in speed cooling and slow cooling area. This process depends on speed of circulated air inside pipes.

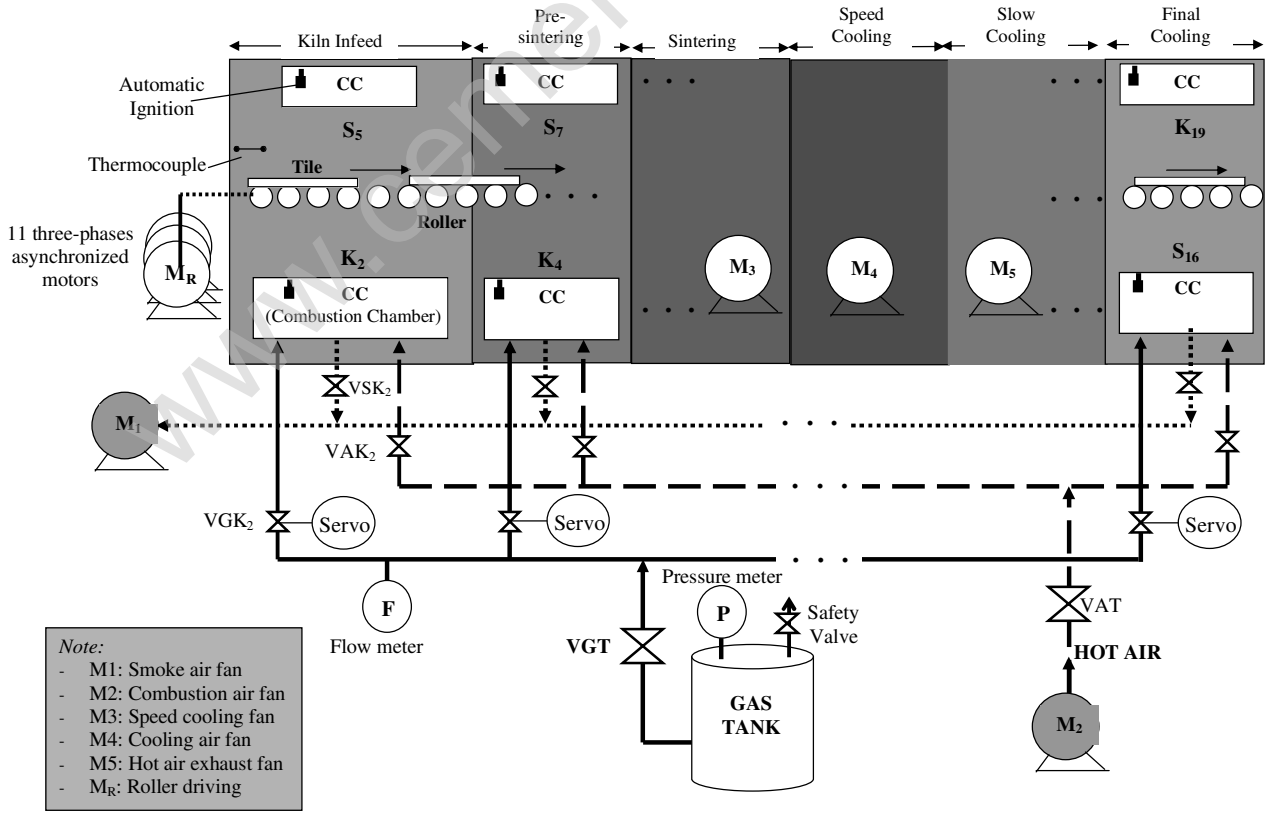

Fig. 3. Graphical representation of ceramic roller kiln.

- Heat exchange between the roller upper area and the roller lower area inside roller kiln.
- Energy loss to environment through cover of kiln.
- Energy loss by smoke air fan (about 3% of generated heat).

Therefore, it is very difficult, even impossible, to build an accurate and perfect mathematical model for temperature process in ceramic roller kiln. In this case, the best way is to use neuro-fuzzy system or NN to build model of this nonlinear process from the collected input–output technical data.

3. Review on ANNs, ANFIS and CANFIS

3.1. Artificial neural networks (ANNs)

The first ideas about NN were introduced by McCulloch and Pitts in 1943 with model of an elementary computing neuron and six years later, Hebb proposed learning rules. After that, ANNs have seen a rapid growth and it has been applied widely in many fields. Besides basic applications such as pattern classification, function approximation, ANNs have been used for identification purpose for linear or nonlinear, multivariable systems. A basic structure of NN comprises of neurons (nodes), interconnections (links) among neurons and weights assigned to these interconnections, threshold (bias) assigned to neurons.

3.2. Adaptive neuro-fuzzy inference systems (ANFIS)

Advantages of fuzzy logic control (FLC) are explicitness and flexibility in linguistic control based on if–then rule set, but problem of determining the shape and location of membership function for each fuzzy variable can be solved by "trial-and-error" method only. Numerical computation, adaptive and learning capability are strong points of NN, however, it is not easy to obtain the optimal structure (number of hidden layer and number of neuron in each hidden layer) of constructed NN and NN also performs numerical rather than symbolic computation. In order to enhance strong points as well as to limit weak points of both approaches, Jang [4,5] combined both FLC and NN to produce a powerful processing tool named NFSs with many representation methods and the most common one is ANFIS. An ANFIS model is an adaptive NN which represents a particular type of fuzzy inference system (FIS). According to [8], there are three types of FIS represented by an ANFIS model as follows:

Type 1 : A FIS whose overall output is the weighted average of each rule's crisp output. The output membership functions are monotonic functions.
Type 2 : A Mamdani FIS where the centroid defuzzification operator is replaced by a discrete version which calculates the approximate centroid of area.
Type 3 : A Sugeno-type FIS whose output is a linear combination of the input variables plus a constant term.

In [6], Jang presented an ANFIS architecture, a special case of Type 3 system, which is briefly explained as following.

Assume that the considered FIS has two inputs (x and y) and one output f. For a first-order Sugeno fuzzy model, a common rule set with two fuzzy if–then rules is as follows:

$$\text{Rule 1 : If } x \text{ is } A_1 \text{ and } y \text{ is } B_1, \text{ then } f_1 = p_1 x + q_1 y + r_1, \tag{1}$$

$$\text{Rule 2 : If } x \text{ is } A_2 \text{ and } y \text{ is } B_2, \text{then } f_2 = p_2 x + q_2 y + r_2, \tag{2}$$

Fig. 4a illustrates the reasoning mechanism for the Sugeno model. The corresponding equivalent ANFIS architecture is shown in Fig. 4b. In this diagram, the output of the ith node in layer l is denoted as $O_{l,i}$

Layer 1: Including adaptive nodes.

$$O_{l,i} = \mu_{Ai}(x) \quad \text{for } i = 1, 2 \tag{3}$$

$$O_{l,i} = \mu_{Bi-2}(y) \quad \text{for } i = 3, 4 \tag{4}$$

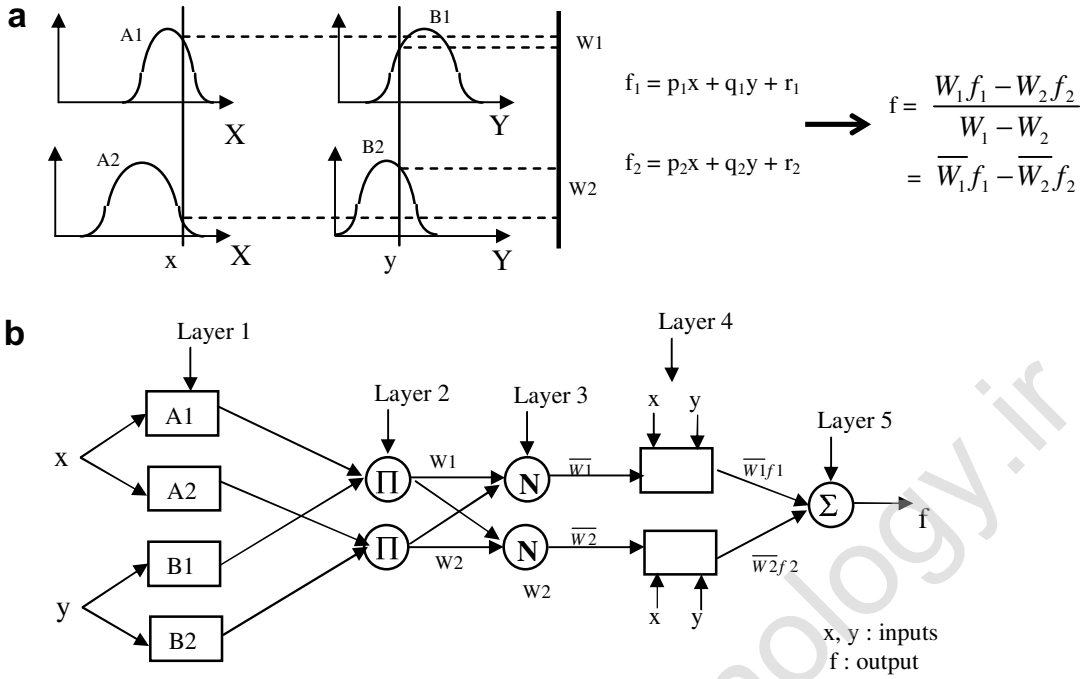

Fig. 4. (a) First-order Sugeno fuzzy model. (b) Equivalent ANFIS architecture.

where

- μ_{Ai} (x) and μ_{Bi-2} (y): any appropriate parameterized membership functions.
- $O_{l,i}$: the membership grade of a fuzzy set A $(=A_1, A_2, B_1$ or $B_2)$ and it specifies the degree to which the given input x (y) satisfies the quantifier A.

Layer 2: Including fixed nodes labeled Π, whose output is the product of all the incoming signals:

$$O_{2,i} = \mu_{Ai}(x)^{*}\mu_{Bi}(y), \quad i = 1,2 \tag{5}$$

Each node output represents the firing strength of a fuzzy control rule.

Layer 3: Including fixed nodes labeled N with function of normalization:

$$O_{3,i} = \overline{w_i} = \frac{w_i}{w_1 + w_2}, \quad i = 1,2 \tag{6}$$

Outputs of this layer are called normalized firing strengths.

Layer 4: Including adaptive nodes.

$$O_{4,i} = \overline{w_i} f_i = \overline{w_i}(p_i x + q_i y + r_i) \tag{7}$$

Layer 5: Including a single fixed node labeled $\sum$ with function of summation.

$$\text{Overall output} = O_{5,1} = \sum_i \overline{w_i} f_i = \frac{\sum_i w_i f_i}{\sum_i w_i} \tag{8}$$

3.3. Coactive neuro-fuzzy inference system (CANFIS)

CANFIS is a generalized ANFIS. CANFIS combines some single-output ANFIS models to produce a multiple-output model with nonlinear fuzzy rules which is an advantage of CANFIS model. There are many ways

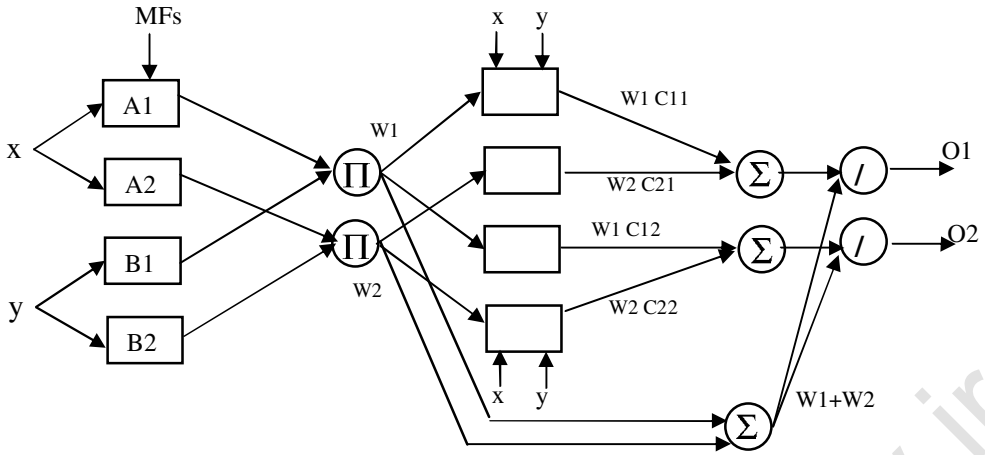

Fig. 5. Two-output CANFIS architecture with two rules per output.

to form a CANFIS from ANFIS and one of them is illustrated in Fig. 5 [6,10]. This diagram is used to maintain the same antecedents of fuzzy rules among multiple ANFIS models. It means that fuzzy rules are constructed with shared membership values to express possible correlations between outputs in this diagram. Besides, we can also form a multiple ANFIS (MANFIS) by placing many ANFIS models side by side, in which, each ANFIS has an independent set of fuzzy rules.

4. The existing applications of NN and NFSs in modeling and control of the single-output nonlinear processes

In fact, NFSs has been popularly used in modeling and control of the nonlinear dynamic processes such as a single link robot manipulator [11], two-link robot [9] or three degrees of freedom robotic manipulator [3]. Besides, NFSs has been also applied largely to many practical industrial processes exhibiting high nonlinearity, for example, two typical complex chemical processes: continuous stirred tank reactor [1,2] and pH neutralization process [2], a coupled-tank liquid-level laboratory process [11], a reduced scale prototype kiln for the ceramic industry [12] or combustion process of a methane–air mixture [7].

In particular, Vieira et al. [12] presented a comparison of ANNs and NFSs applied for modeling a reduced scale prototype kiln for the ceramic industry, which is nonlinear and working under measurement noise. Through NN and Fuzzy Logic Toolboxes in MATLAB software, the direct and inverse models of kiln temperature process were developed by using ANNs as well as ANFIS in the first-order and second-order approaches. The detailed results are summarized in Table 1.

Efe and Kaynak [3] investigated the identification ability of nonlinear systems by using feed-forward neural networks (FNN), Radial basis function neural networks (RBFNN) and ANFIS. In their paper, identification mechanisms are studied and performances are comparatively evaluated for a three degrees of freedom robotic manipulator. The angle error of each approach for base, shoulder, elbow of manipulator were plotted. These comparisons are summarized in Table 2.

Table 1
Comparison between ANNs and ANFIS in modeling stage

Modeling stage		ANNs	ANFIS (single output)
Precision of model (using MSE criterion in training and testing sets)		High	Low
Complexity of model	No. of parameters	Smaller	Much larger
	No. of training epochs	Larger	Smaller
	Training time	Smaller	Larger

Table 2
Comparison among FNN, RBFNN and ANFIS

Performance measures	FNN	RBFNN	ANFIS (single output)
Tracking performance	Low	Low	High
Pre-training time	Low	High	Low
Operational simplicity	High	High	Medium
Expert knowledge incorporation	Low	Medium	High

5. Process control of ceramic tile roller kiln

As we know that ceramic tile is comprised of two main parts, glaze and biscuit, in which, biscuit is enameled with a thin glaze layer on its surface (Fig. 6a). Therefore, the required operating temperature for upper locations (used to fire for glaze part), such as S_5, S_7, S_9, S_{11}, S_{13}, S_{15}, K_{17}, K_{19} points (Fig. 8), should be different from that for lower locations (used to fire for biscuit part), such as K_2, K_4, S_6, S_8, S_{10}, S_{12}, S_{14}, S_{16} points. Moreover, the required operating temperature value in roller kiln also changes depending on the considered area along roller kiln (consisting of six areas of roller kiln as shown in Fig. 2). In general, the designed reference temperatures of roller kiln are complicated and these temperature values need to be followed strictly and accurately, otherwise many serious defects will occur on the finished product. Let us consider the cooling areas (speed cooling and slow cooling areas as shown in Fig. 3) in roller kiln, if the operating temperatures in these areas do not follow the correspondent set-point values during cooling phase, then there are two possibilities. The first is the shrinkage of biscuit is higher than that of glaze (Fig. 6b) and the second is the shrinkage of biscuit is lower than that of glaze (Fig. 6c). In both cases, this problem will lead to the deformation of the finished tile called planarity defect. Besides, many other defects such as insufficient firing and overfiring, tonality variations of the glaze, size variations and black heart also relate closely to performance of temperature process in roller kiln. Therefore, the accurate and perfect control for temperature process in roller kiln is essential.

5.1. Modeling the MIMO nonlinear temperature process of roller kiln

In this research, we followed following steps for modeling of the MIMO nonlinear temperature process in ceramic roller kiln:

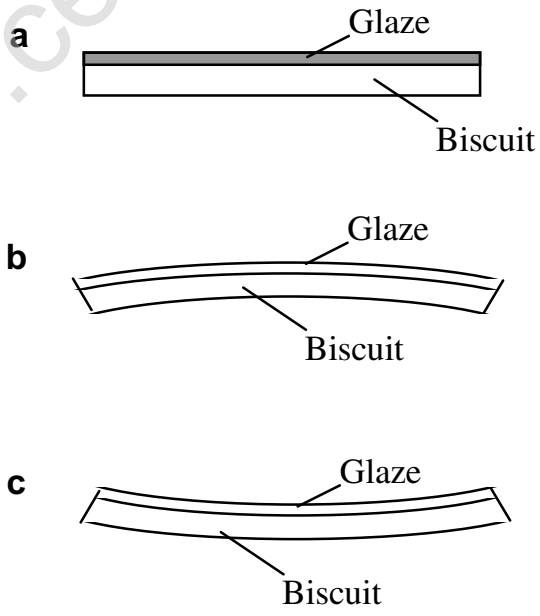

Fig. 6. Two parts of ceramic tile: glaze and biscuit. (a) Normal situation. (b) When the shrinkage of biscuit is higher than that of glaze (during cooling phase). (c) When the shrinkage of biscuit is lower than that of glaze (during cooling phase).

- Selection of input and output variables.
- Collecting input–output technical data from real system.
- Training ANNs models.
- Training CANFIS models.
- Comparison between these two models about root mean squared error (RMSE), training time, complexity of architecture.

5.1.1. Selection of input and output variables

After investigating the collected data as well as the kiln diagram and discussions with kiln engineers, we propose that the performance of temperature process in roller kiln can be modeled with 16 inputs and 22 outputs (multi-outputs). Inputs are the opening level of controlling valves and outputs are the real temperature values at various points along roller kiln as shown in Fig. 7.

The actual inputs and outputs locations in the real system are as follows (Fig. 8):

- 16 inputs (Opening level of controlling valves): S_5, S_7, S_9, S_{11}, S_{13}, S_{15}, K_{17}, K_{19}, K_2, K_4, S_6, S_8, S_{10}, S_{12}, S_{14}, S_{16}.
- 22 outputs (Real temperature values at various areas): KV_{22}, KP_{21}, K_1, K_3, S_5, S_7, S_9, S_{11}, S_{13}, S_{15}, K_{17}, K_{20}, K_{19}, K_2, K_4, S_6, S_8, S_{10}, S_{12}, S_{14}, S_{16}, K_{18}.

where S_i, K_i with $i = \{1,22\}$: Measuring points are equipped with temperature sensors and gas valves. The most important six points are S_{10}, S_{11}, S_{12}, S_{13} (gas valves in sintering area of roller kiln), K_{17} (used for speed cold air fan) and K_{19} (used for hot air fan).

5.1.2. Collecting input–output technical data from real system

Collecting the input–output technical data from ceramic tile manufacturing factory was carried out for temperature parameters (real values and set-point ones) in all areas of roller kiln. The total number of collected

Fig. 7. Input and output variables of studied model.

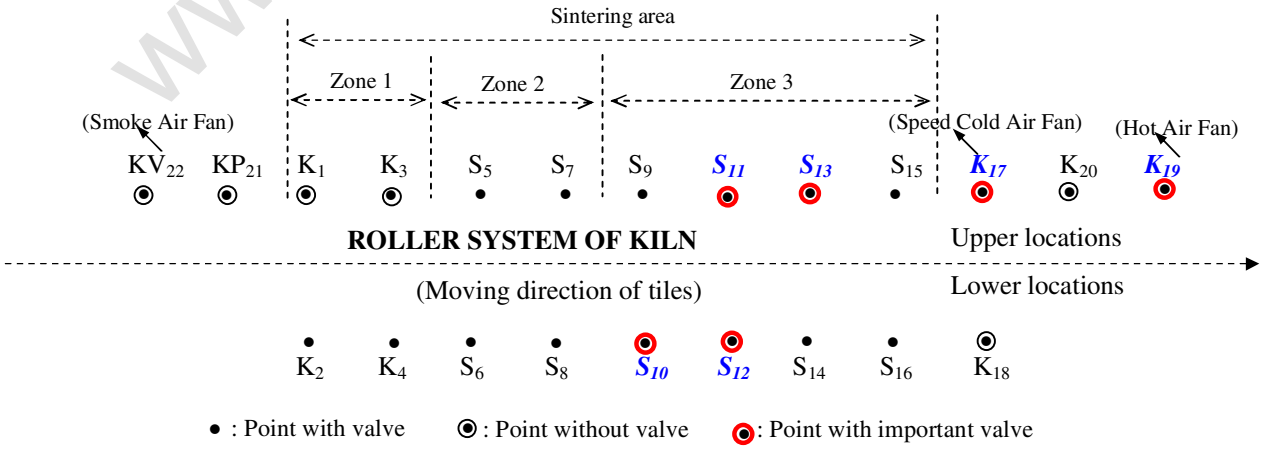

Fig. 8. Controlling valve location diagram at various areas in roller kiln.

data sets is 285. The data is normalized before being used for simulation. Sample of collected data is shown in Fig. 9.

Some notations used in Fig. 9 are SP (set-point value of temperature (°C)), RV (real value of temperature (°C)), S_i and K_i (the same definition as part 5.1.1 above).

Here, we choose the interval [0.05, 0.95] to carry out the normalization process for the collected data as follows:

Pre-processing:

$$X'_t = \frac{0.95(X_t - a)}{A - a} + 0.05 \tag{9}$$

Post-processing:

$$X_t = \frac{(A - a)(X'_t - 0.05)}{0.95} + a \tag{10}$$

where X_t is the actual value; a is the minimum value of X_t; A is the maximum value of X_t; X'_t is the transformed value.

5.1.3. Modeling of the kiln temperature process

5.1.3.1. Modeling using ANNs. In NN designing process, the optimal structure of NN (the right number of hidden layer as well as the right number of neuron in each hidden layer) can be found out by "trial-and-error" method only. More layers can give a better fit, but the training takes longer. Too few neurons give a poor fit, while too many neurons result in over-training of the net [2].

In this work, training NN models from the collected data patterns was performed by using WinNN32 software. Here, we used 5-layers feed-forward NN which was trained by back-propagation training algorithm to get the model of real plant. Results obtaining using the developed NN models with 5 layers are summarized in Table 3.

For 9-10-13-11-9 NN structure, we elaborate detailed results as follows:

RMSE is used to evaluate performance of developed model. RMSE can be calculated using Eq. (11).

$$\mathrm{RMSE} = \mathrm{MSE}^{1/2} = \left[\frac{1}{N}\sum_{i=1}^{N}(y_i - \hat{y}_i)^2\right]^{1/2} \tag{11}$$

where N is the number of data, y_i is the ith actual output, and $\hat{y}_i$ is the ith model output.

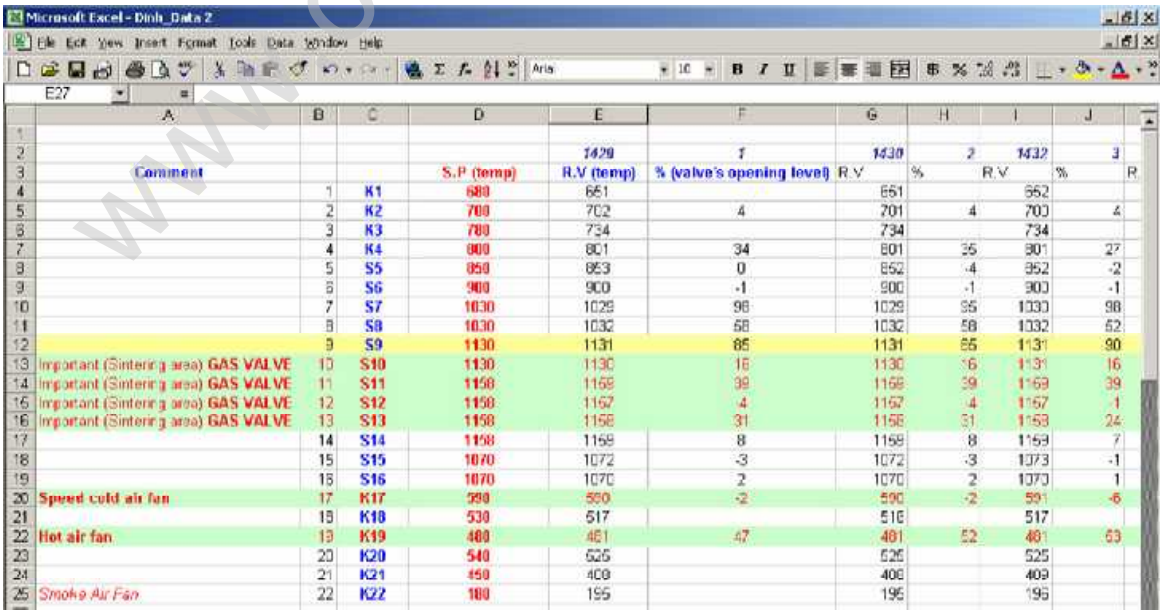

Fig. 9. Sample of collected data for ceramic roller kiln temperature.

Table 3
Developed NN models

Structure of NN models		RMSE	No. of epoch	Target error	No. of weights and biases
6 inputs – 6 outputs	6 – 9 – 14 – 10 – 6	1.0679	74865	0.01	419
	6 – 14 – 18 –12 – 6	1.14136	40,135	0.01	674
	6 – 18 – 22 –16 – 6	1.0678	30,610	0.01	1014
8 inputs – 8 outputs	8 – 15 – 20 – 10 – 8	1.24	24,310	0.01	753
	8 – 10 – 15 – 12 – 8	1.2385	39,085	0.01	551
	8 – 12 – 18 – 10 – 8	1.2386	29,835	0.01	620
9 inputs – 9 outputs	9 – 12 – 15 – 10 – 9	1.3136	211,675	0.01	574
	9 – 14 – 18 – 15 – 9	1.3578	24,775	0.01	839
	9 – 10 – 13 – 11 – 9	1.374	50,065	0.01	505

Based on the graph in Fig. 10, we can conclude that in the interval from iteration number 0 to iteration number 1600, RMSE value goes down quickly, this is a good performance because we know that smaller value RMSE gets, better model we obtain. After that, RMSE value keeps stable at constant 1.374 when number of iterations continue increasing in the training process.

Pattern error is the difference between real output value and desired output value of NN. According to the curve in Fig. 11, we can see that although the pattern error often oscillates but the main trend of curve is going down first and then keeping constant when number of iterations increases during NN training process. Besides, architecture diagram of 9-10-13-11-9 NN is shown in Fig. 12.

From plot of weight distribution in Fig. 13, we can know exactly the number of weights and biases in developed NN. In this case, there are 505 weights and biases. From that, we also know how complicated the studied model is. The numerical values of weights and biases of the obtained model are stored in a weight file that is automatically produced as soon as the training process finished.

5.1.3.2. Modeling using CANFIS. Constructing and simulating neuro-fuzzy models from the collected data patterns was carried out using NeuroSolution software. All developed CANFIS models used the generalized

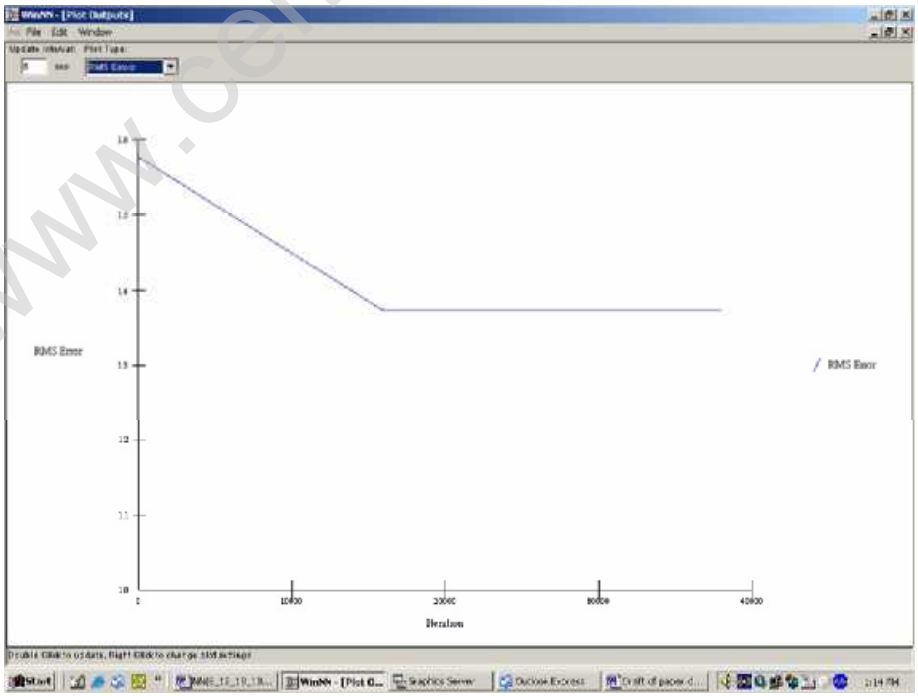

Fig. 10. Plot of RMSE value of modeled NN.

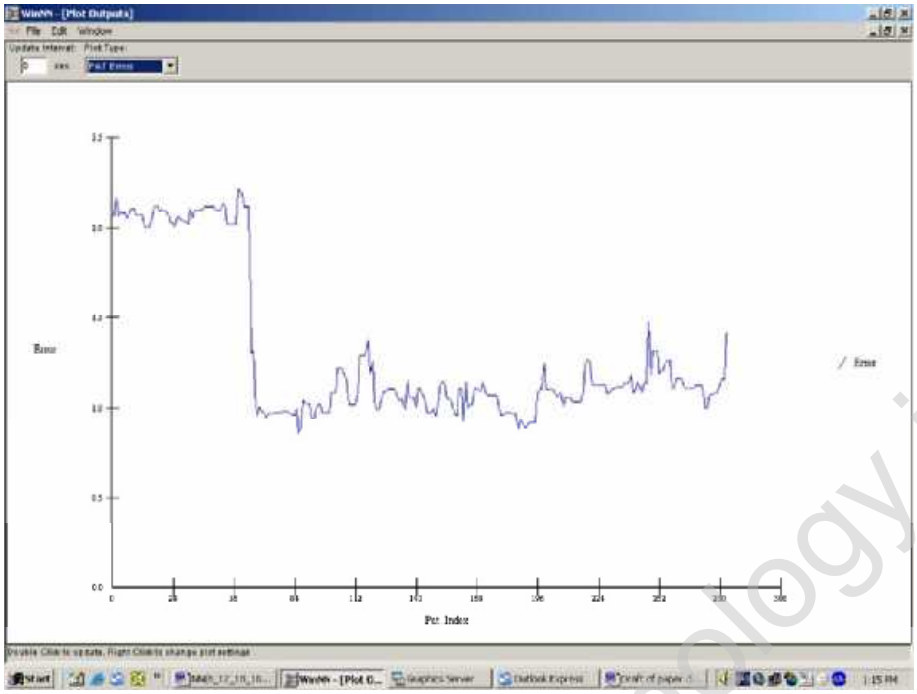

Fig. 11. Plot of pattern error for modeled NN.

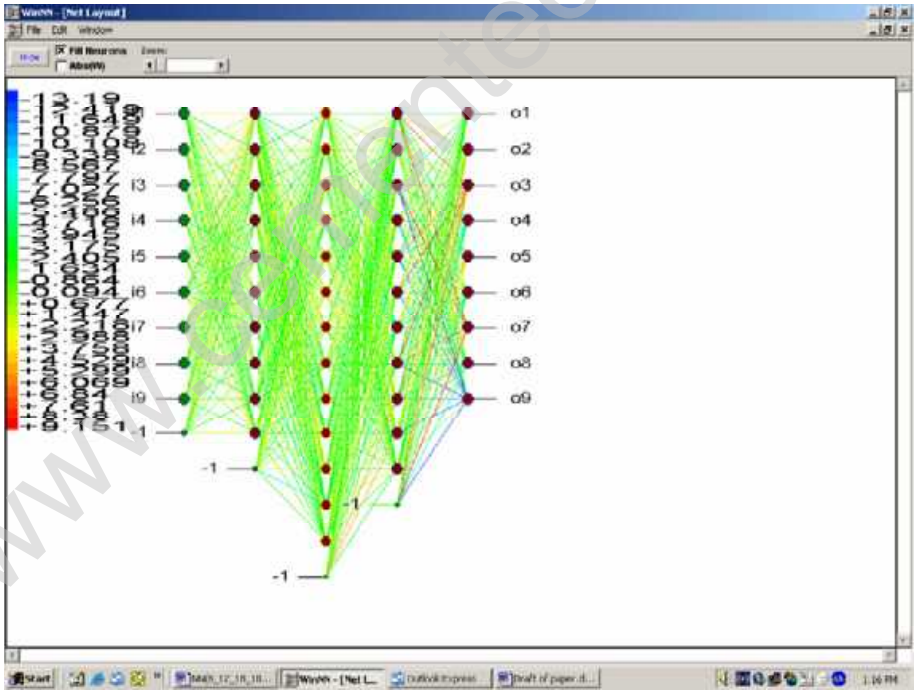

Fig. 12. Architecture diagram of modeled NN.

bell membership function (MF) with three MFs per input and TSK fuzzy model proposed by Takagi, Sugeno and Kang for fuzzy part in these hybrid systems. Simulation results of CANFIS models are summarized in Table 4.

In the first case, a CANFIS model is developed with 6 inputs – 6 outputs which are the most important inputs and outputs in temperature process of roller kiln. They are six valves including four gas valves in Zone

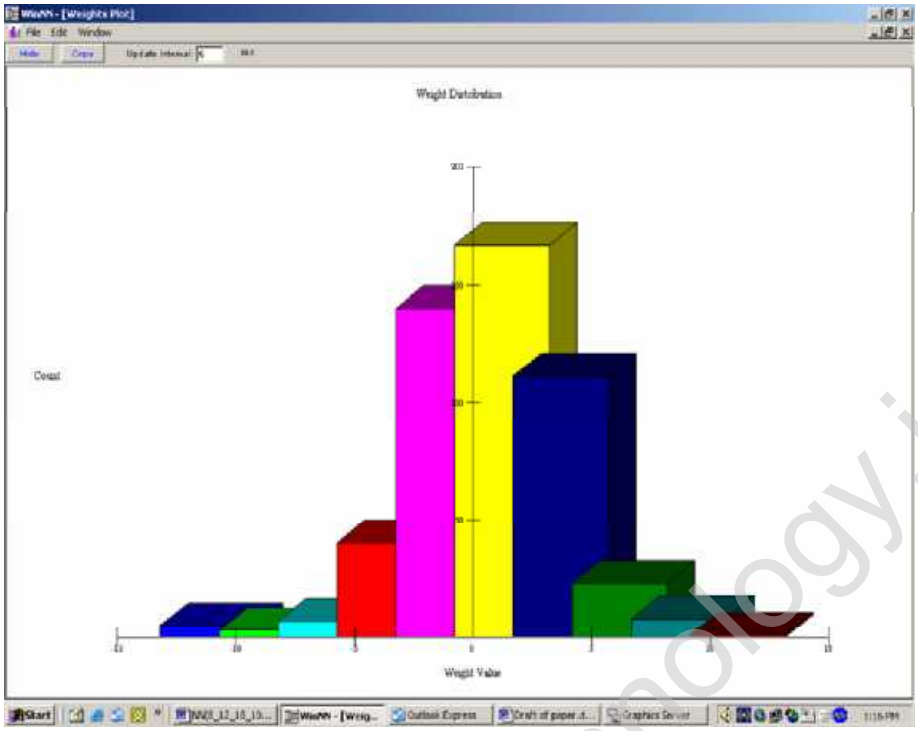

Fig. 13. Plot of weight distribution of modeled NN.

Table 4
Developed CANFIS models

Structure of CANFIS model	RMSE	No. of epoch	Target error	No. of weights and biases
6 inputs – 6 outputs	0.140876	2000	0.01	17,586
8 inputs – 8 outputs	0.166445	2000	0.01	210,088
9 inputs – 9 outputs	0.177243	1000	0.01	708,750

3 of sintering area (S_{10}, S_{11}, S_{12}, S_{13}), one valve used to control speed cold air fan (K_{17}) and one valve used to control hot air fan (K_{19}) (see Fig. 8). Of which, the first four valves are used to supply most of the heat for temperature process of roller kiln, and the last two valves are used to control the energy loss in roller kiln. In other words, the opening levels of these six valves decide almost all temperature values in the whole roller kiln. In the second case, the number of input and output is increased to 8 (adding S_{14}, S_{16}) in order to obtain a CANFIS model with higher accuracy for the kiln temperature process. Moreover, 9 input – 9 output CANFIS model (adding S_{15}) is also simulated by using NeuralBuilder in NeuroSolution software. These three CANFIS models were trained by momentum learning rule during the training process so that we can get the global minimum value of performance index MSE. In the case of 9 inputs – 9 outputs CANFIS model, we show the detailed results in Fig. 14.

5.1.3.3. Comparison of NN and CANFIS models. Criterions used for comparing between NN and CANFIS models are RMSE values, the actual training time and complexity of architecture.

By comparing the obtained results for three cases of multi-output system viz, 6 inputs – 6 outputs, 8 inputs – 8 outputs and 9 inputs – 9 outputs, we can see that although structure of CANFIS models is more complicated than NN models (with the same number of layers) due to the larger number of weights and biases (obtained from the statistical data) and the actual training time of CANFIS models is much longer than NN models, accuracy level in modeling of CANFIS is much better than NN because RMSE values in the case of CANFIS models are around seven times smaller than NN values. Using this we can conclude that for mod-

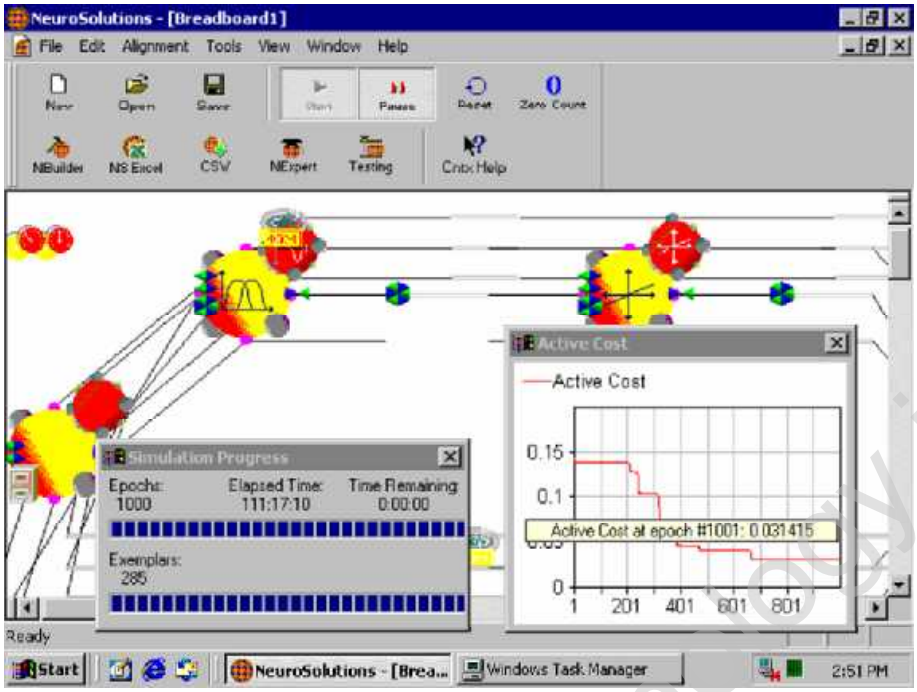

Fig. 14. The 9 inputs – 9 outputs CANFIS model of process. This model used the generalized bell membership function and momentum (MOM) learning rule during training process. The training time for this model is 111:17:10 h. The curve at the right corner shows the changing of active cost (MSE value) during 1000 epochs training process and the final MSE value we obtained is 0.031415 (minimum value), from that, value of RMSE is calculated as 0.177243.

eling a MIMO nonlinear process like temperature in roller kiln in ceramic tile manufacturing industry, CANFIS architecture is the better approach to model the physical behaviours of the studied plant.

Due to the limitation of the PC hardware used (RAM capacity of 1 GB), we cannot obtain CANFIS model with the desired number of real plant outputs (22 outputs). However, it does not introduce a significant bias to the developed model compared with real plant because the most important valves (S_{10}, S_{11}, S_{12}, S_{13}, K_{17} and K_{19}) which decide almost all temperature values in the whole ceramic roller kiln, are already used in training process for all NN and CANFIS models.

From above comparison, we can draw a conclusion that modeling a MIMO nonlinear process like temperature process of ceramic roller kiln with CANFIS has a better accuracy than modeling with NN because CANFIS has more complicated architecture but smaller RMSE value. Therefore, CANFIS model is selected for use in the next control phase.

6. Controlling the MIMO nonlinear temperature process of ceramic roller kiln

6.1. Designing real-time controller

6.1.1. Reasons for selecting feed-forward NN controller

Here we selected NN controller because, for this type of controller, when the set-point values change, outputs of controller will change properly. From that, outputs of process (real temperature of ceramic roller kiln) also change correctly and track the reference value accurately. Besides, because this is real-time controller that requires fast responding time, working time of controller is the most important factor. Therefore, we chose the feed-forward NN model for designing this real-time controller.

6.1.2. Model of process

Here we use CANFIS model with 6 inputs – 6 outputs. Due to limitation of the used software, in the case of CANFIS model, when Dynamic Link Library (DLL) is exported, we cannot use CANFIS model with larger

number of input/output (such as 8 inputs – 8 outputs or 9 inputs – 9 outputs model) for identifying MIMO nonlinear temperature process in roller kiln. The CANFIS model of this process was designed and trained using NeuroSolutions 5.02 software as shown in Fig. 16. In this model, the training process has been carried out with momentum learning rule in 200 epochs. The numerical output data of model was stored in BST file that was automatically produced when the training process finished. This file contains not only the value of weights and biases but also the input file and desired file used for training process. After that, these output data was used during control phase for block "Process" as shown in block diagram in Fig. 15.

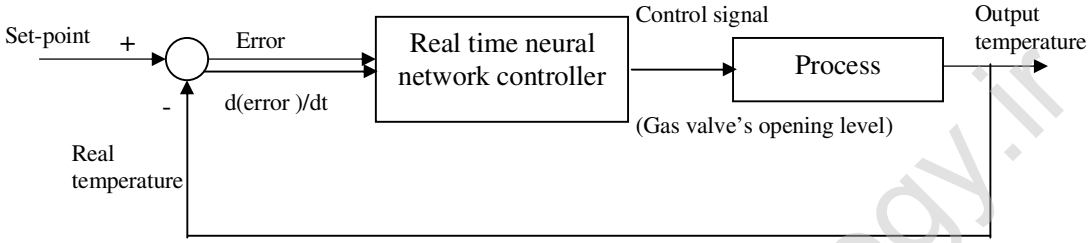

Fig. 15. Block diagram of real time control.

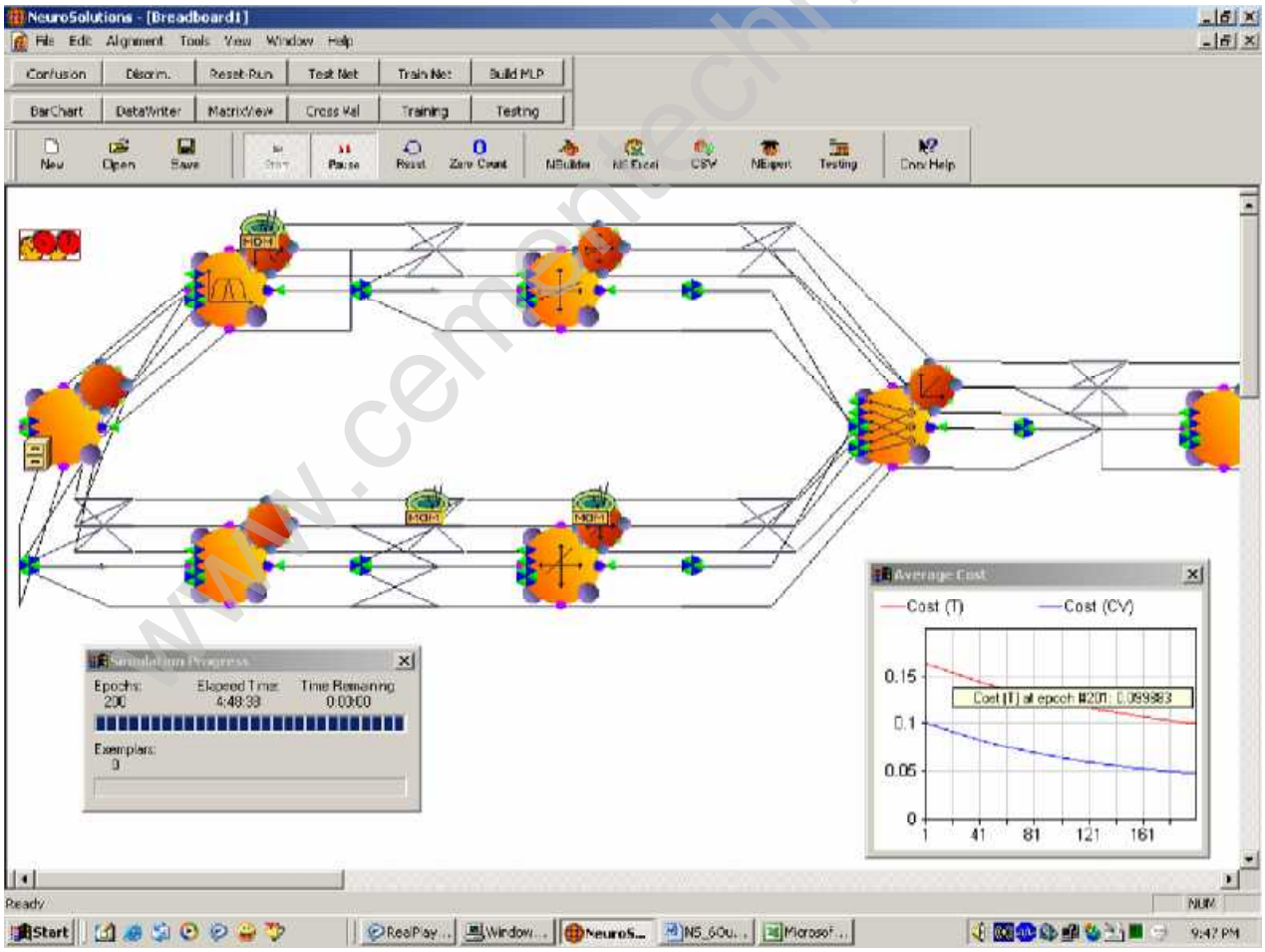

Fig. 16. The 6 inputs – 6 outputs CANFIS model of process during training process. The network and axons (nodes) illustrated for the designed CANFIS model with 5 layers. In this model, the generalized bell membership function and momentum (MOM) learning rule were used. The training time for this model is 4:48:38 h. In the plot window located at right corner, the upper curve is for MSE value during training process and the lower one is for MSE value during cross validation process.

6.1.3. NN controller architecture

Because we already use 6 inputs – 6 outputs CANFIS model for process modeling, model of controller will comprises of 12 inputs (for error of temperature and the rate of change of error d(error)/dt). Here, a 12-9-6 feed-forward NN model is used for controller. During the training process for this model, we used momentum learning rule in 1000 epochs so that we can find out the global minimum value of performance index. In this case, the used performance index is MSE. In total of 285 data patterns collected from real system, we used 28 patterns (10%) for cross validation and 257 patterns (90%) for training process of NN controller. This NN controller has been designed and trained in NeuroSolutions 5.02 software as shown in Fig. 17.

6.2. Simulation results for controller's performance

After NN controller is designed and trained, we need to test the controller's performance when it is used for the feedback control as shown in Fig. 15.

After model of process and controller were built with identified architecture, weight and bias values, we exported DLL with the chosen project type of Visual C++ 6. From that, we obtained project shell in Visual C++ with three main classes: NSNetwork, NSLearningNetwork and NSRecallNetwork. In which, NSLearningNetwork class is used for training network, NSRecallNetwork class is used for recalling network and NSNetwork is the parent class for above two classes.

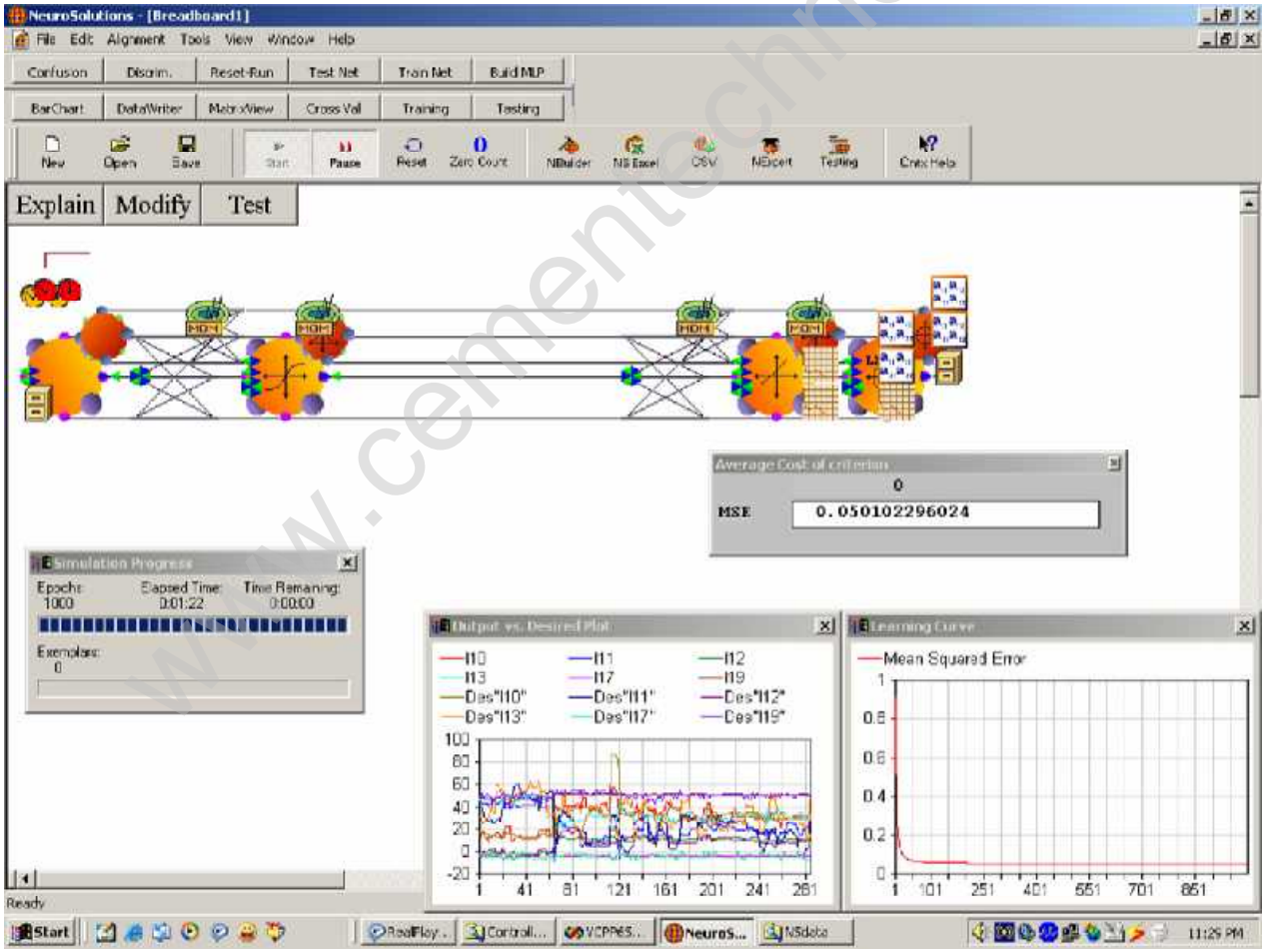

Fig. 17. The 12-9-6 feed-forward NN model for controller during training process. The network and axons illustrated for the designed NN model with 3 layers (input layer, hidden layer and output one). The momentum (MOM) learning rule was used for training this model. The final MSE value of 0.0501 and its curve during 1000 epochs training process were also displayed in this diagram. This training process took 1:22 min. The plot window showed the changing of output and desired values of all six outputs in different color curves. (For interpretation of the references to colour in this figure legend, the reader is referred to the web version of this article.)

During testing process, since model of process and controller are already trained, we do not need to use NSLearningNetwork class, we just used functions belonging to NSRecallNetwork class to recall and get output of controller as well as of process. In Fig. 15, while outputs of controller are exactly inputs of process, outputs of process (the real temperatures of roller kiln), after being compared with set-point values, become two types of input for controller, they are error of temperature and the rate of change of error d(error)/dt.

In Visual C++ project, in order to create some necessary function buttons in interface, we modified and added source codes for some files such as header file and C++ file. Finally, we obtained an interface shown in Fig. 18.

From this interface, we get output of process (the real temperatures of roller kiln) at six most important considered points along roller kiln. These points are S_{10}, S_{11}, S_{12}, S_{13}, K_{17} and K_{19}. For example, we can get the normalized output data of process as shown in Fig. 19 when input of process is taken from a collected data pattern. After that, this data will be converted into the unnormalised format and then compared with set-point values in order to produce error of temperature and d(error)/dt. These two parameters are inputs to the controller. Controller's output data is the input of process and once again, we get the real temperatures of roller kiln in normalized format at six considered points as illustrated by Fig. 20.

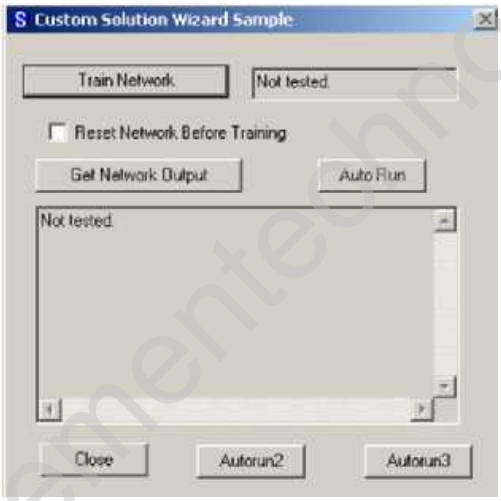

Fig. 18. The interface and function buttons created in Visual C++ project.

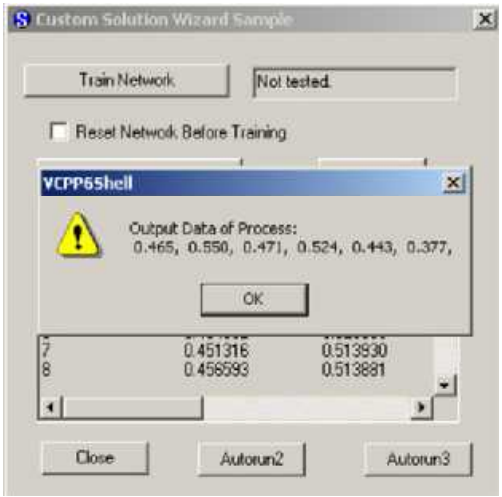

Fig. 19. The normalized output data of process obtained at first test (for first set-point temperature set).

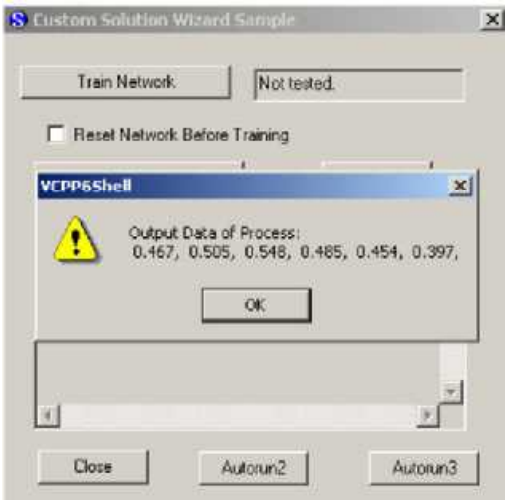

Fig. 20. The normalized output data of process obtained at second test (for first set-point temperature set).

7. Discussion

When changing type of product in ceramic tile manufacturing line, the required set-point temperature set of roller kiln changes accordingly. Therefore, we considered three real different set-point temperature sets, in this study, named first set-point temperature set, second set-point temperature set and third set-point temperature set. Actually, the testing process in part 6.2 above was repeated two times more for second set-point temperature set and third set-point temperature set. After the outputs of process are converted into unnormalised format, we can summarize the numerical data of the real temperatures in roller kiln, when roller kiln is controlled by the designed NN controller, as Table 5 and charts in Figs. 21–23.

From these data, we can calculate the percentage error between the real values and set-point ones of the temperature in roller kiln for three cases of set-point temperature set as shown in Table 6.

From this table, we can see that the maximum percentage error between real values and set-point ones of temperature in roller kiln for three cases of set-point temperature set is 1.000091%. Actually, this is the maximum steady-state error of the real temperature. Meanwhile, the typical steady-state error bound in control field is, normally, 2% or 5% [13,14]. Therefore, we can see that percentage error 1.000091% is reduced and is acceptable in controlling process for temperature of ceramic roller kiln. Due to this very good performance of the designed NN controller, the temperature values in roller kiln can track the changed set-point temperature values accurately and therefore, the finished product's defects coming from variation of temperature in ceramic roller kiln can be limited significantly.

Table 5
Numerical data of temperature in roller kiln during testing process according to three real different set-point temperature sets

Considered point in roller kiln	S_{10}	S_{11}	S_{12}	S_{13}	K_{17}	K_{19}
	1	2	3	4	5	6
First set-point temperature set (°C)	**1130**	**1158**	**1158**	**1158**	**590**	**480**
Real temperature at first test (°C)	1130.368	1151.895	1167.636	1150.983	590.2411	482.0979
Real temperature at second test (°C)	1130.389	1151.184	1169.581	1150.326	590.2758	482.2874
Second set-point temperature set (°C)	**1130**	**1149**	**1179**	**1149**	**590**	**480**
Real temperature at first test (°C)	1130.368	1148.632	1178.216	1148.994	590.2411	480.0326
Real temperature at second test (°C)	1130.389	1148.395	1178.621	1148.747	590.2758	480.0958
Third set-point temperature set (°C)	**1130**	**1146**	**1174**	**1146**	**590**	**480**
Real temperature at first test (°C)	1129.747	1146.579	1173.886	1145.996	589.8274	481.3768
Real temperature at second test (°C)	1129.756	1146.437	1174.048	1145.832	589.8505	481.4611

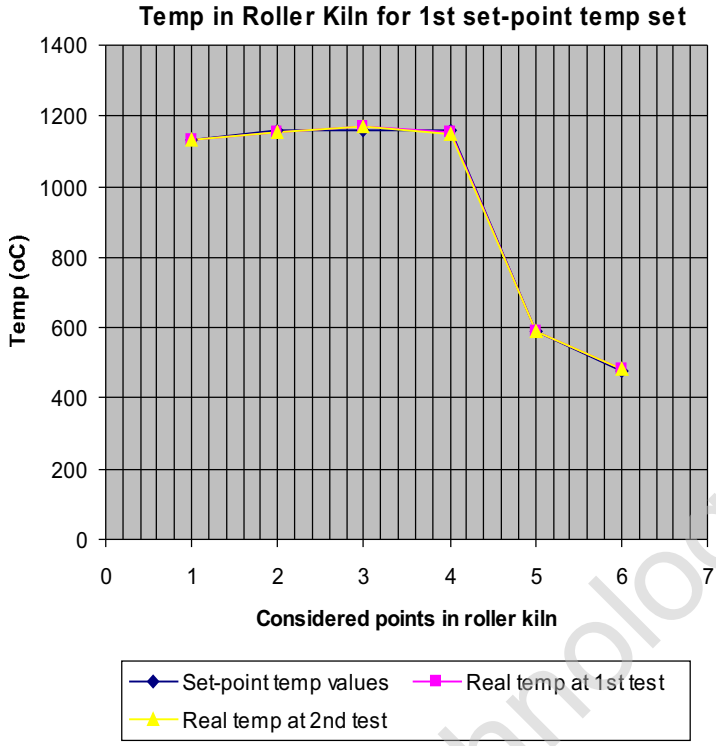

Fig. 21. Chart of temperature in roller kiln during testing process (for first set-point temperature set).

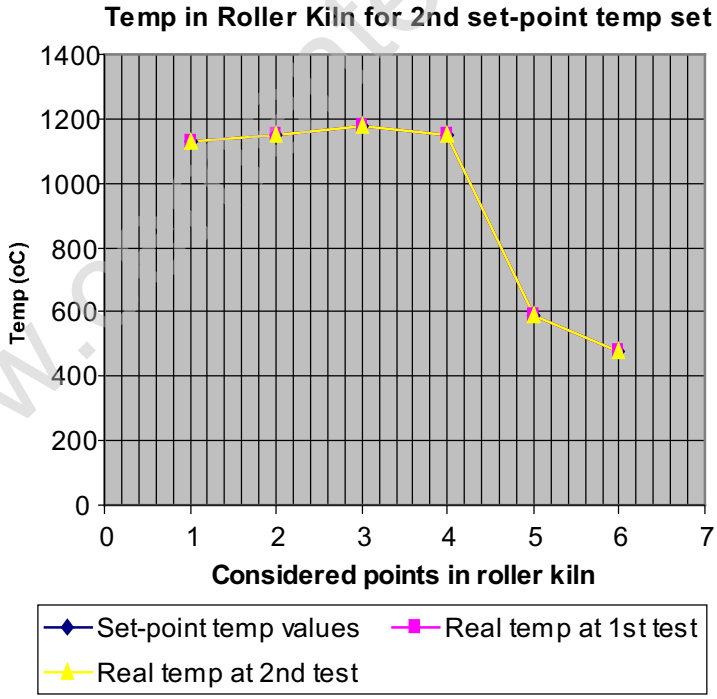

Fig. 22. Chart of temperature in roller kiln during testing process (for second set-point temperature set).

In this case, we do not need to calculate the temperature values during transient response because ceramic roller kiln, in fact, works continuously without break at the required operating temperatures. Normally, there will be an one or two weeks annual maintenance period for ceramic roller kiln to maintain devices. After this period is finished, roller kiln will be restarted for operating. At that time, roller kiln's temperatures will start at

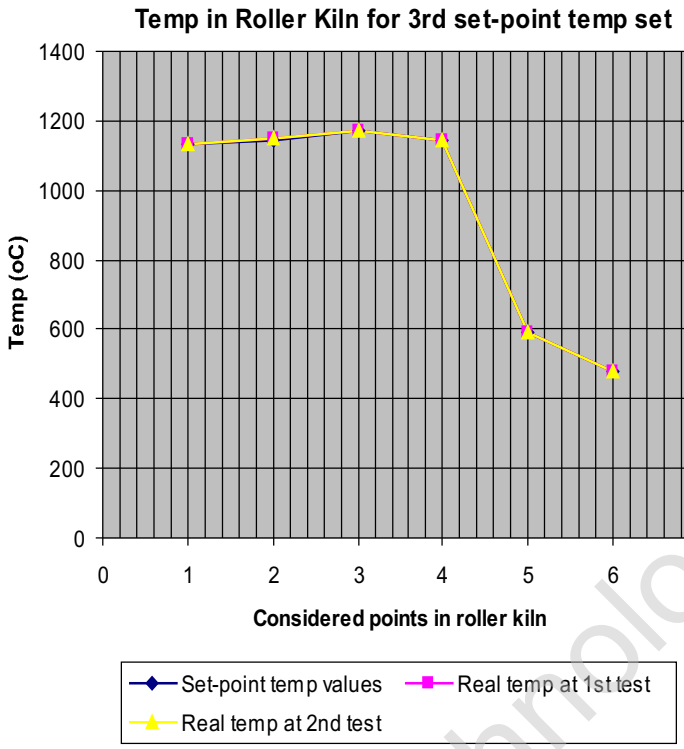

Fig. 23. Chart of temperature in roller kiln during testing process (for third set-point temperature set).

Table 6
Data of the percentage error between the real values and set-point ones of temperature in roller kiln for three cases of set-point temperature set

Considered point	S_{10}	S_{11}	S_{12}	S_{13}	K_{17}	K_{19}
	1	2	3	4	5	6
First set-point temperature set (°C)	**1130**	**1158**	**1158**	**1158**	**590**	**480**
Error at first test (%)	0.032604	0.527225	0.832106	0.605945	0.040856	0.437061
Error at second test (%)	0.034467	0.588583	1.000091	0.662667	0.046744	0.476535
Second set-point temperature set (°C)	**1130**	**1149**	**1179**	**1149**	**590**	**480**
Error at first test (%)	0.032604	0.032064	0.066515	0.00055	0.040856	0.006798
Error at second test (%)	0.034467	0.052677	0.032141	0.021987	0.046744	0.019956
Third set-point temperature set (°C)	**1130**	**1146**	**1174**	**1146**	**590**	**480**
Error at first test (%)	0.022357	0.050519	0.009683	0.000367	0.02926	0.286842
Error at second test (%)	0.021612	0.038119	0.004124	0.014696	0.025335	0.304386

ambient temperature and then increase. When the real temperatures in roller kiln reach the required operating values, roller will start rotating to transport ceramic tile into roller kiln and sintering procedure will be started. Or in other words, in all possible cases, ceramic tile is sintered in roller kiln only when the temperature values in roller kiln already stabilized around the steady-state values. Therefore, we do not need to analyse roller kiln's temperature values during transient phase.

8. Conclusions

In this paper, description, analysis, role and function, physical behaviours as well as technical specifications related to temperature process in a real ceramic roller kiln were introduced. From the study we concluded that this temperature process not only is a MIMO nonlinear process but also is too complicated to build a mathematical model for identification purpose. This work focused on exploring MIMO feature in modeling and

control of a real industrial nonlinear process using simulation. Basically, this work comprises of two separate parts. The first one is comparative study between NN and CANFIS model to find out better approach for identifying a complicated MIMO nonlinear process like temperature process of ceramic roller kiln. This comparison was carried out by simulation with the conclusion that CANFIS method is better suited for modeling the studied plant. In the control part, a feed-forward NN controller has been designed and trained using the process data collected from the real system. We created Visual C++ project to test the controller performance. The numerical data we got from the testing process showed that the designed NN controller is reliable when the roller kiln set-point temperature set changes. The accuracy obtained for the controller is high and error is smaller than reported in the literature. However the limitation so far is that all the results are obtained by simulation and in future we are planning to test the model and controller for a pilot ceramic kiln plant.

Acknowledgements

The authors would like to express our sincere thanks to COSEVCO ceramic tile manufacturing factory in Vietnam for their help during technical data collection for this research.

References

[1] A. Aoyama, F.J. Doyle, V. Venkatasubramanian, A fuzzy neural network approach for nonlinear process control, International Journal of Engineering Applications of Artificial Intelligence 8 (5) (1995) 483–498.
[2] R. Babuška, H. Verbruggen, Neuro-fuzzy methods for nonlinear system identification, Annual Reviews in Control (2003) 73–85.
[3] M.O. Efe, O. Kaynak, A comparative study of neural network structures in identification of nonlinear systems, Mechatronics 9 (8) (1999) 287–300.
[4] J.-S.R. Jang, Neuro-fuzzy modeling: architecture, analyses and applications, Dissertation, Department of Electrical Engineering and Computer Science, University of California, Berkeley, CA 94720, 1992.
[5] J.-S.R. Jang, ANFIS: adaptive-network-based fuzzy inference system, IEEE Transactions on Systems, Man and Cybernetics 23 (3) (1993) 665–685.
[6] J.-S.R. Jang, C.-T. Sun, E. Mizutani, Neuro-Fuzzy and Soft Computing: A Computational Approach to Learning and Machine Intelligent, Prentice-Hall International, 1997.
[7] J. Kim, N. Kasabov, HyFIS: adaptive neuro-fuzzy inference systems and their application to nonlinear dynamical systems, Journal of Neural Networks 12 (1999) 301–1319.
[8] H.F. Kwok, D.A. Linkens, M. Mahfouf, G.H. Mills, Rule-base derivation for intensive care ventilator control using ANFIS, Journal of Artificial Intelligence in Medicine 29 (2003) 185–201.
[9] W.-S. Lin, C.-H. Tsai, J.-S. Liu, Robust neuro-fuzzy control of multivariable systems by tuning consequent membership functions, Journal of Fuzzy Sets and Systems 124 (2001) 181–195.
[10] E. Mizutani, J.-S.R. Jang, Coactive neural fuzzy modeling, Proceedings of International Conference on Neural Networks (1995) 760–765.
[11] T.L. Seng, M. Khalid, R. Yusof, S. Omatu, Adaptive neuro-fuzzy control system by RBF and GRNN neural networks, Journal of Intelligent and Robotic Systems 23 (1998) 267–289.
[12] J. Vieira, F.M. Dias, A. Mota, Artificial neural networks and neuro-fuzzy systems for modeling and controlling real systems: a comparative study, International Journal of Engineering Applications of Artificial Intelligence 17 (3) (2004) 265–273.
[13] H. Bishop Robert et al., The Mechatronics Handbook, CRC Press, ISA – the Instrumentation, Systems and Automation Society, 2002, pp. 25–13.
[14] S. Levine William et al., The Control Handbook, CRC Press, IEEE Press, 1996, p. 158.